# Static quadrupolar perturbed NMR in structurally incommensurate systems. II. $^{87}Rb$ satellite transitions in $Rb_2ZnBr_4$

R. Walisch and J. Petersson
*Fachbereich Physik, Universität des Saarlandes, D-6600 Saarbrücken, Federal Republic of Germany*

J. M. Perez-Mato
*Departamento de Fisica, Facultad de Ciencias, Universidad del Pais Vasco, Apartado 644, Bilbao, Spain*
(Received 16 May 1986)

The $^{87}Rb$ NMR $m=\pm\frac{1}{2}\leftrightarrow m=\pm\frac{3}{2}$ satellite transitions are studied in a detailed manner in the normal, incommensurate, and commensurate phases of high-quality $Rb_2ZnBr_4$ single crystals. By these means, an experimental method is realized for investigating local phenomena related to structural phase transitions which is considerably more direct and sensitive than the $m=+\frac{1}{2}\leftrightarrow m=-\frac{1}{2}$ central transition, which, so far, has been used nearly exclusively in NMR studies of $Rb_2ZnBr_4$ and its isomorphous. In the normal phase the electric-field-gradient tensor (EFG) at the Rb sites is determined by the well-known Volkoff method. The widths of the frequency distributions appearing in the incommensurate phase, which generally show some centers of intensity and, particularly, edge singularities, depend strongly on both the temperature and crystal orientation. The temperature dependence is measured for special crystal orientations, where one crystallographic axis is parallel to the direction of the static magnetic field, while for special temperatures, for which the plane-wave limit holds, the orientational dependence is investigated in detail. On passing to the low-temperature commensurate phase, the spectra of the incommensurate phase merge into the discrete lines corresponding to the structure of that phase. The degeneracies and symmetries of the NMR rotation patterns in the incommensurate phase are discussed without any special model on the basis of the general symmetry properties of that phase as described in the preceding work. The data can be fitted quantitatively by a general Fourier series for the EFG. On the contrary, the "local" model, which previously has often been applied, fails to describe both the orientational and temperature dependences of the NMR spectra. The observed temperature dependences are related to the temperature dependence of the order parameter of the incommensurate phase. The present results exclude the strong floating of the modulation waves reported previously in another work.

## INTRODUCTION

Among the crystals exhibiting incommensurate (IC) phases, isomorphous $Rb_2ZnBr_4$ and $Rb_2ZnCl_4$, henceforth abbreviated as RZB and RZC, respectively, have been studied extensively by applying various experimental methods. Both crystals undergo a second-order transition from a paraelectric normal (N) phase to an incommensurate phase at $T_i$. At a lower temperature $T_c$, a lock-in transition occurs to a ferroelectric commensurate (C) phase, whose unit cell is tripled along the $c$ direction of the high-temperature *Pcmn* structure. In the IC phase a one-dimensional modulation occurs along that direction whose wavelength is not commensurate with the underlying high-temperature lattice. The phase transition temperatures are $T_i\approx 75\,^{\circ}C$, $30\,^{\circ}C$, and $T_c\approx -75\,^{\circ}C$, $-80\,^{\circ}C$ for RZB and RZC, respectively. Thus, broad incommensurate phases occur in both crystals in temperature regions very favorable for experimental investigations.

It has been shown by numerous works that high-frequency spectroscopy can give some valuable insight into the local phenomena related to the phase transitions in these substances. Particularly quadrupolar perturbed nuclear magnetic resonance (NMR) of the $^{87}Rb$ nucleus ($I=\frac{3}{2}$) sensitively probes local phenomena via the interactions of the electric-field-gradient tensor (EFG) at the Rb site with the quadrupole moment of the nucleus. Nearly all studies known employ the shift of the $m=\frac{1}{2}\leftrightarrow m=-\frac{1}{2}$ central transition which is related to the EFG in a perturbation-theory approach by second-order effects. According to our knowledge, the $m=\pm\frac{1}{2}\leftrightarrow m=\pm\frac{3}{2}$ satellite transitions have not been studied so far in RZB, whereas a previous work[1] showed that the satellites can be detected in all phase of high-quality RZC single crystals. It is, however, highly desirable to investigate the satellite transitions more systematically because of the following reasons. Since in a perturbation theory the satellite transitions are related to the EFG by first-order effects, they are about 2 to 3 orders of magnitude more sensitive to the changes of the EFG than the central transtion. Moreover, the satellites are related to the EFG in a very direct manner. One measures a certain component of the EFG in the laboratory frame. This does not hold for the second-order shift of the central transition which is determined in a more complicated manner by a quadratic form in the components of the EFG. Finally, it is well known that even a small number of crystal imperfections may broaden the satellites to such a considerable extent that they cannot be detected. Therefore, the detectability or nondetectability of the satellites is

 

a strong hint at the crystal quality. This fact is of special importance for investigating IC phases because these phases are well known to be sensitively influenced by crystal imperfections. In view of these arguments it is surprising that so few works study the IC phases in RZB and RZC via the satellite transitions of the $^{87}$Rb nucleus. One may suspect that the poor signal-to-noise ratio which occurs in the IC phase particularly near $T_c$ (Ref. 1) and the fact that crystals of minor quality were used, constitute the main reasons for this situation.

In the following, we shall present what we believe to be the first detailed study of the $^{87}$Rb NMR satellite transitions in RZB. It will be shown that the satellites can be detected in all phases, thus providing a sensitive tool for investigating the local properties of this substance. With reference to the preceding publication[2] (henceforth abbreviated as I), the results will be interpreted in terms of the symmetries of the various phases of RZB including the superspace symmetry of the IC phase. As a central result, it will be shown that the experiments cannot be understood on the basis of the so-called "local" model. This model has been previously applied in order to describe NMR data of IC phases, particularly for explaining the observed behavior of the central line in RZB.[3–5] That "nonlocal" terms are relevant for the EFG expansion was proposed earlier in Refs. 6–8. Subsequently, these effects could be detected also by $^{14}$N NMR in $(NH_4)_2ZnCl_4$ (Ref. 9) and $[N(CH_3)_4]_2ZnCl_4$ (Ref. 10). A "nonlocal" model has been introduced in Ref. 11 in the case of studies of the central line in RZB. We shall apply a general Fourier series of the EFG as given in I. As discussed therein, this Fourier series coincides with the "nonlocal" EFG expansion in Ref. 12 if the system is in the plane-wave limit. Our results will be discussed also in relation to those of previous studies[4,5] of the $^{87}$Rb NMR central transition in RZB and to those of our previous work on $^{87}$Rb satellites in RZC.[1]

## II. EXPERIMENTAL DETAILS

Since high-quality RZC single crystals could be grown from aqueous solutions,[1] we employed this procedure also in the present case. Single crystals of RZB were grown in the IC phase at about 40 °C and in the N phase at about 80 °C from aqueous solutions of RbBr and $ZnBr_2$ with the molar ratio 2:1. The high-temperature crystal-growth apparatus was constructed because it was suspected that a crystal grown in the "distorted" IC phase contains more imperfections than a crystal grown in the N phase.[4] This supposition, however, could not be confirmed by our experimental results: We could not detect any difference between crystals grown at 40 °C and 80 °C. The samples used in the NMR experiments had a volume of about 0.6 cm$^3$ and were orientated by goniometric methods.

The NMR equipment used was described previously.[1,13] Special apparatus was available which rendered it possible to rotate the sample around an axis perpendicular to the static magnetic field $H_0$ and to incline the probe head by small angles with respect to the axis of the cryomagnet. By that means, the orientation of the sample with respect to the static magnetic field could be adjusted very accurately. This is a necessary condition to be fulfilled by the equipment since the $^{87}$Rb satellite transitions depend sensitively on the orientation of the sample.

A standard gas-flow temperature-regulation unit was used with a temperature stability of about ±0.1 K over the measuring period. The temperature was measured by a small NiCr-Ni thermocouple located at a distance of 2–4 mm from the sample. The temperature gradient over the sample volume was less than 1.5 K.

## III. EXPERIMENTAL RESULTS

### A. N phase

Defining the crystal axes in such a way that $a > c > b$ holds for the lattice constants, the space group of the N phase is $Pcmn$.[14] In the N phase there are two different kinds of Rb nuclei termed Rb(1) and Rb(2). The nuclei of one particular kind are related to each other by symmetry operations. Each kind is made up of four nuclei in the unit cell. The EFG components $V_{xz}$ of equal magnitude but opposite sign belong to Rb nuclei which are connected to each other by the glide planes $c_x$ perpendicular to the $a$ axis or by the glide planes $n_z$ perpendicular to the $c$ axis. Since all Rb nuclei lie in the mirror planes $m_y$ perpendicular to the $b$ axis, the elements $V_{xy}$ and $V_{yz}$ vanish and, thus, one principal axis of the EFG is directed along the crystallographic $b$ axis. Therefore, taking also into account the Laplace condition $V_{xx}+V_{yy}+V_{zz}=0$, the complete EFG tensor can be determined applying the well-known Volkoff formalism[15] on a rotation of the crystal around the $b$ axis which is perpendicular to the direction of the magnetic field $H_0$ ($b$ rotation). Accordingly, one obtains for the first-order splitting of the satellites for that rotation

$$\Delta\nu_y = K_y + L_y\cos(2\theta_y) - C_y\sin(2\theta_y)\ , \tag{1}$$

where $\theta_y = \sphericalangle(\mathbf{c},\mathbf{H}_0)$, $K_y=(\phi_{zz}+\phi_{xx})/2$, $L_y=(\phi_{zz}-\phi_{xx})/2$, $C_y=\phi_{xz}$, and $\phi_{ij}=V_{ij}eQ/h$. As usual, we denote by $V_{ij}$ a component of the EFG tensor, by $eQ$ the quadrupole moment of the Rb nucleus and by $\phi_{ij}$ a component of the EFG quadrupole coupling tensor. From Fig. 1 one then readily obtains (in MHz): $\phi_{xx}=-0.180$, $\phi_{yy}=-4.330$, $\phi_{zz}=4.510$ and $\phi_{xz}=\pm0.225$ for Rb(1) and $\phi_{xx}=-3.115$, $\phi_{yy}=0.765$, $\phi_{zz}=2.350$, and $\phi_{xz}=\pm0.080$ for Rb(2), where the accuracy is better than ±0.010 MHz. Thus, the angles are small which occur between the principal directions of the EFG lying in the mirror planes $m_y$ and the crystallographic $a$ and $c$ axes. They are ±2.7° for Rb(1) and ±0.8° for Rb(2). These values fit nicely to those previously derived[5] and not so well to those obtained by Rutar *et al.*[4], both works using the second-order shift of the $^{87}$Rb central line. Because of the reasons discussed above in the introduction, our data are presumably much more accurate. For both EFG's one element in the main diagonal is small compared to the other two. This result, which reflects the symmetry of the charge distribution around the Rb nucleus, is analogous to that derived previously[1] for RZC.

Of course, the symmetries of the $^{87}$Rb EFG's in RZB

and RZC reflect the crystal symmetry. $[N(CH_3)_4]_2ZnCl_4$ has the same space group in the high-temperature phase as RZB and RZC with the N nuclei located in the mirror plane. Therefore, the rotation patterns of $^{14}N$ ($I=1$) quadrupole splittings reported recently[10] should show the same symmetries as those of the $^{87}Rb$ transitions in RZB and RZC. Since this is not the case, these results[10] can be understood only by assuming a misorientation of the sample. Particularly in the notation of that work, the *a*-rotation pattern does not show the necessary symmetry of our Fig. 1 and because of symmetry in both the *b*- and *c*-rotation patterns instead of the four curves given only two curves should be present (compare, e.g., to Fig. 1 in Ref. 1). Such misorientations may give rise to incorrect EFG's and, more important, to complicated rotation patterns of the spectra in the IC phase which can hardly be interpreted correctly.

*Note added in proof.* The corresponding corrections of these results will be published by the authors of Ref. 10 in a forthcoming publication in Z. Naturforsch.

### B. Temperature dependence of the $^{87}Rb$ spectra for special crystal orientations

For Rb(2) with the crystal orientation $\mathbf{a}\|\mathbf{H}_0$ and for Rb(1) with $\mathbf{b}\|\mathbf{H}_0$ the satellite transitions could be detected in the entire IC phase and for Rb(2) with $\mathbf{b}\|\mathbf{H}_0$ in the upper part of the IC phase. The results are summarized in Figs. 2–6.

On passing from the N to the IC phase for Rb(2) with $\mathbf{a}\|\mathbf{H}_0$ (Figs. 2 and 3) one line splits into a typical incommensurate distribution of frequencies with edge singularities. The distribution width strongly increases on lowering the temperature, the type of the spectra not being altered over a large temperature range. Near $T_c$ the satellite transition which above $T_i$ in the N phase gives rise to a single line with a width of about 2–3 kHz reaches a distribution width of about 600 kHz. About 10 K above the lock-in transition at $T_c$ additional centers or maxima of intensity become visible besides the edge singularities. According to the symmetry elements of the space group

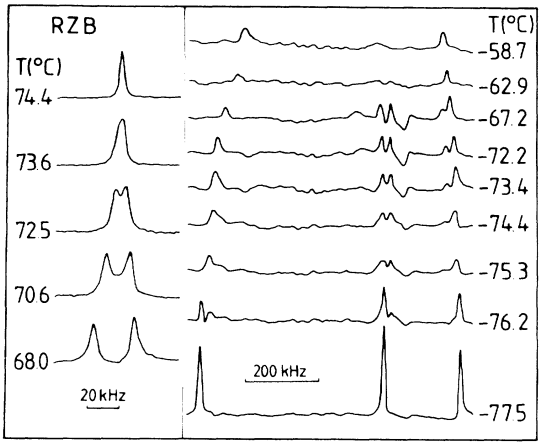


FIG. 2. Spectra of the lower frequency satellite of Rb(2) in the crystal orientation $a\|H_0$ near $T_i$ (left) and $T_c$ (right).

$Pc2_1n$ of the C phase and the tripling of the unit cell along the *c* direction three narrow discrete lines are detected below $T_c$ in the orientation under consideration, thus demonstrating the correct orientation of the sample with respect to the direction of $H_0$ also at low temperatures. In the small temperature range investigated below $T_c$ the frequencies of these C lines apparently depend linearly on the temperature. Their temperature dependence is the more pronounced the larger the distance from the line in the N phase. At $T_c$ the outermost maxima of intensity of the IC spectra merge into the outermost C lines in a continuous manner. The additional centers of intensity, which can be seen approximately in the middle part of the IC spectra, merge into the middle C line. Since the intensity of the irradiation signal diminishes toward the edges of the spectra, the intensities of the outer lines detected below $T_c$ (Fig. 2) appear smaller than the intensity of the middle C line. Actually the intensities are equal. This was verified by irradiating exactly in the middle between two lines to be compared. The same holds

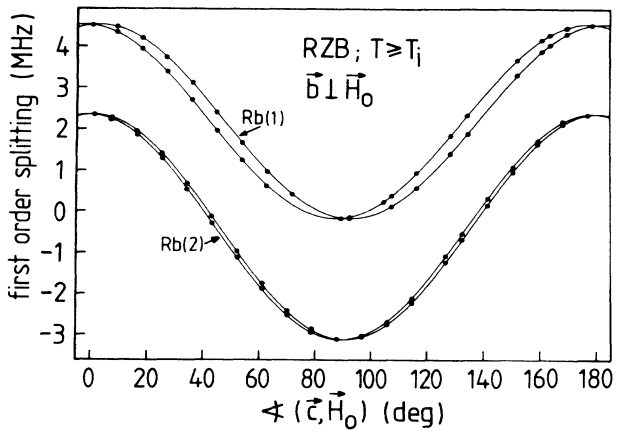


FIG. 1. Rotation pattern of the $^{87}Rb$ satellite line splittings in the N phase of RZB near $T_i$. Fit curves according to (1).

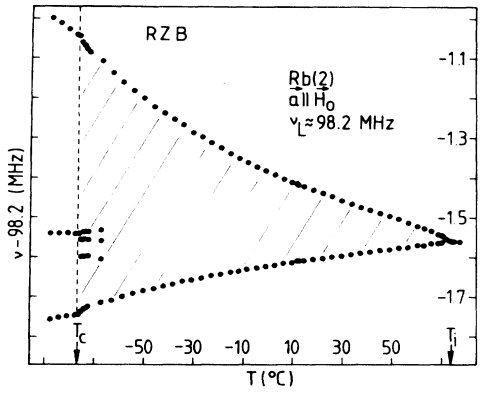


FIG. 3. Temperature dependence of the frequency of one satellite transition of Rb(2) at $a\|H_0$. The points indicate the frequencies of the discrete lines in the N and C phase and the centers of intensity in the IC phase. The dashed area represents the background spectrum in the IC phase.

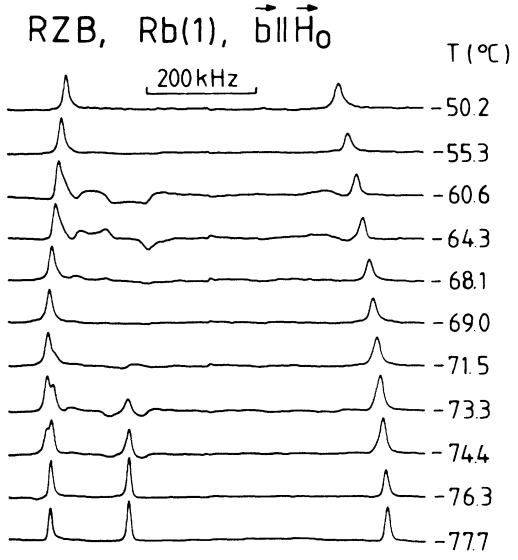


FIG. 4. Spectra of the upper frequency satellite of Rb(1) in the crystal orientation $b||H_0$ near $T_c$.

for the Rb(1) spectra described below. Because of the extreme width of the spectra phase distortions, i.e., a mixing of absorption parts with dispersion parts of the signal, could not completely be avoided (see Figs. 2 and 4). This argument applies to most spectra recorded in the IC phase. By that, information on the accurate line shape including the incommensurate background is lost.

The spectra described so far were obtained on lowering the temperature step by step. The satellite transitions of Rb(1) with $\mathbf{b}||\mathbf{H}_0$ were measured changing the temperature in the opposite direction from the C to the N phase. On the whole, the results are similar to those obtained for Rb(2) with $\mathbf{a}||\mathbf{H}_0$ (Figs. 4 and 5). There are, however, some discrepancies in a temperature interval of about 15 K above $T_c$. Only about 5 K above $T_c$ the additional intensity maxima vanish which are located near the center of the spectrum. Surprisingly, at about $-65$ ° C and $-60$ °C again structures appear in the IC spectra in addition to the edge singularities. In the same temperature region, the spectra of the $^{87}$Rb central transition recorded in the same temperature run showed a slight additional deformation as well. On further heating, only the edge singularities remain as centers of intensity in the IC satellite spectra. At $T_i$ they merge into the discrete line of the N phase.

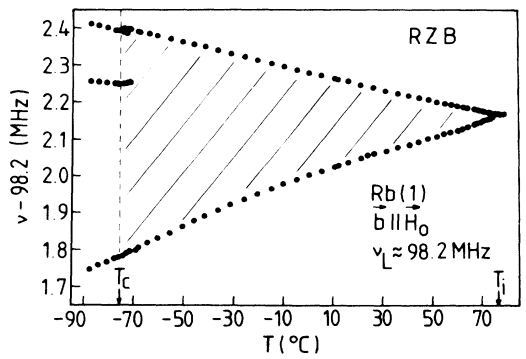


FIG. 5. Same as Fig. 3, except for Rb(1), $b||H_0$.

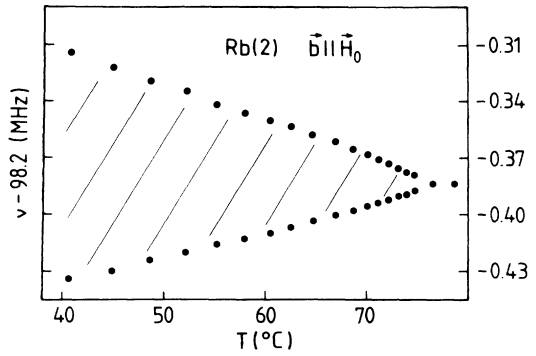


FIG. 6. Temperature dependence of the frequency of one satellite transition of Rb(2) at $b||H_0$ in the N phase near $T_i$ and the upper part of the IC phase. The symbols have the same meaning as in Fig. 3.

At the same crystal orientation the satellite transitions of Rb(2) were detected only in the upper part of the IC phase because of the problems which arise from the overlap with the central line. According to Fig. 6 again two edge singularities of the incommensurate frequency distribution merge into a discrete line at $T_i$. Contrary to the two cases discussed so far the splitting of the two edge singularities is nearly symmetrical with respect to the line of the N phase.

In the C phase at about $-81$ °C (just below $T_c$) both satellite transitions were measured for all Rb nuclei with $\mathbf{a}||\mathbf{H}_0$ and $\mathbf{b}||\mathbf{H}_0$. At these orientations the first-order splittings directly give the absolute values of the components $\phi_{xx}$ and $\phi_{yy}$. For the three nonsymmetry-related Rb sets of the C phase which stem from the Rb(1) of the N phase we obtain (in MHz) $|\phi_{xx}| = 0.449$, 0.610, and 0.088; $|\phi_{yy}| = 4.790$, 4.484, and 3.493. For the remaining Rb sets of the C phase related to Rb(2) of the N phase we obtain $|\phi_{xx}| = 3.081$, 3.500, and 2.055; $|\phi_{yy}| = 1.037$, 1.072, and 0.209. In both cases, of course, we do not know in which way these components are associated with each other.

### C. Rotations in the IC phase

For a commensurate crystal lattice the EFG at the site of a certain nucleus usually can be determined from the dependence of the satellite transitions on the crystal orientation (see, e.g., Fig. 1). Therefore, one would expect that some hints can be obtained on the EFG at the Rb sites in the IC phase from measuring the orientational dependence of the spectra in that phase. The spectra of the upper frequency satellite transition of Rb(1) were detected on rotating the crystal around $\mathbf{c}\perp\mathbf{H}_0$ apart from the crystal orientation $\mathbf{b}||\mathbf{H}_0$ by small angles (small $c$-rotation pattern) at ambient temperature. The results are presented in Fig.

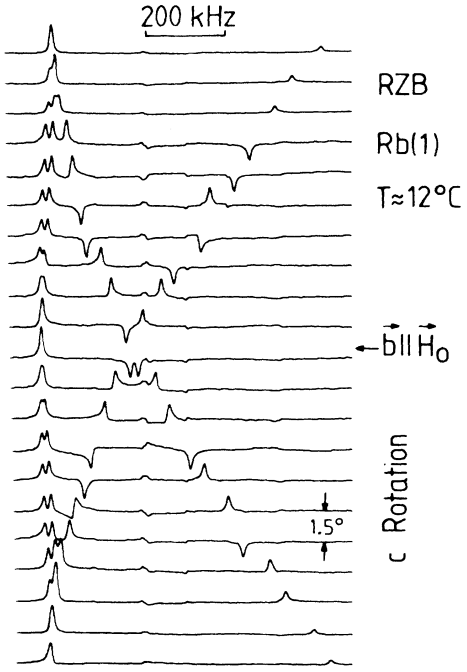


FIG. 7. Orientational dependence of the spectra of the upper frequency Rb(1) satellite for a $c$ rotation ($c \perp H_0$) near the crystal orientation $b \| H_0$ in the IC phase at about 12 °C. The spectra are normalized.

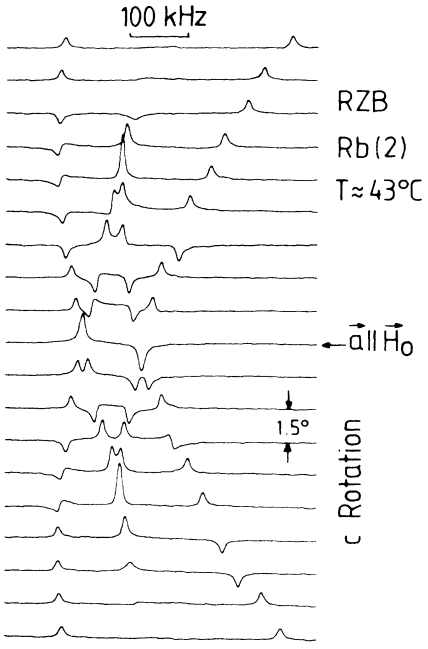


FIG. 9. Orientational dependence of the spectra of the upper frequency Rb(2) satellite for a $c$ rotation ($c \perp H_0$) near the crystal orientation $a \| H_0$ in the IC phase at about 43 °C. The spectra are normalized.

7. On the left-hand side there is a singularity, the frequency of which is essentially independent of the rotation angle and which splits into two singularities for some angles of rotation around ±6°. Moreover, two other singularities emerge from the singularities at the left-hand side at angles of rotation of about ±14° and move to the right-hand side showing a stronger orientational dependence and intersecting at $\mathbf{b} \| \mathbf{H}_0$ (compare also to Figs. 4 and 5). The symmetry of the spectra with respect to this crystal orientation is obvious.

All other rotational dependences were measured at about 43 °C, i.e., about 30 K below $T_i$ where the plane wave limit can be assumed to hold. Comparing the results of Figs. 7 and 8, some variations with temperature

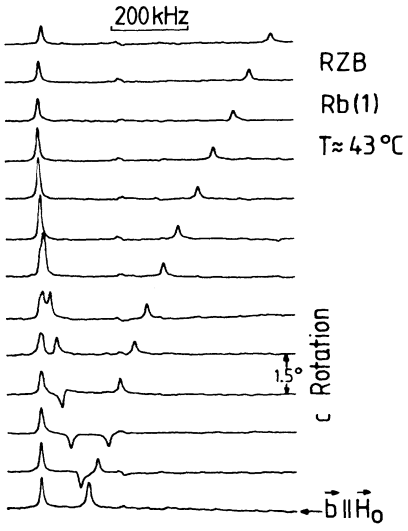


FIG. 8. Same experiment as given in Fig. 7 at about 43 °C.

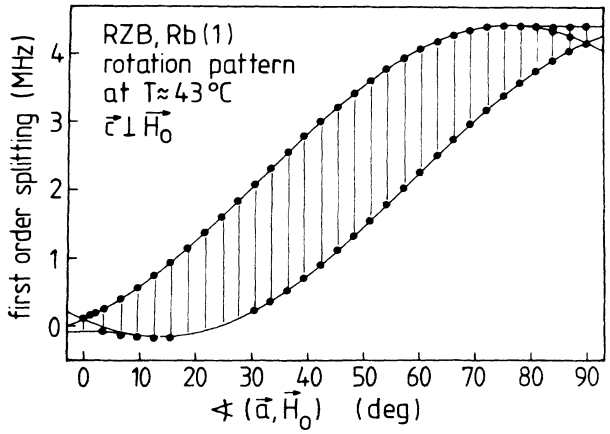


FIG. 10. Pattern of $c$ rotation between the crystal orientations $a \| H_0$ and $b \| H_0$ of the $^{87}Rb$ satellite splittings of the singularities observed for Rb(1) in the IC phase at 43 °C. The vertical lines between the edge singularities indicate the widths of the incommensurate spectra.

become obvious. So, e.g., the angle of rotation at which in Fig. 8 the inner singularity merges into the outermost one amounts only to about 10°. Moreover, whereas in Fig. 7 the singularity at the left-hand side splits in a certain orientation range in Fig. 8 only a small broadening of that singularity can be detected.

The results presented in Fig. 9 also demonstrate the symmetry of the spectra with respect to a crystal orientation where one axis is parallel $H_0$ (in this case $\mathbf{a}\|\mathbf{H}_0$). Rotating the crystal apart from the orientation $\mathbf{a}\|\mathbf{H}_0$, each of the two edge singularities which are observed in that orientation (compare to Figs. 2 and 3) of the crystal, split into two. At increasing angle of rotation the two inner singularities are moving toward each other, coincide and finally disappear in the incommensurate background spectrum at angles of rotation of about ±13°. The two outermost edge singularities show a strong dependence on the crystal orientation and can be observed for all rotation angles.

Because of the symmetries observed for the satellite spectra with respect to the crystal orientations $\mathbf{a}\|\mathbf{H}_0$ and $\mathbf{b}\|\mathbf{H}_0$ it suffices for determining the complete angular dependence for a $c$ rotation to measure the spectra in the angular regime of 90° between $\mathbf{a}\|\mathbf{H}_0$ and $\mathbf{b}\|\mathbf{H}_0$. The corresponding rotation patterns of the first-order splittings of the satellite singularities are presented for Rb(1) and Rb(2) in Figs. 10 and 11, respectively. (Here the term splitting is a generalization of the usual meaning. We take the distance of the corresponding singularities of the upper and lower satellite; cf. discussion in Sec. V.) In both cases the frequency range between the outermost edge singularities contains the incommensurate background spectrum. Thus, both Figs. 10 and 11 demonstrate that the IC spectra are comparatively narrow in the crystal orientations $\mathbf{a}\|\mathbf{H}_0$ and $\mathbf{b}\|\mathbf{H}_0$ (compare Figs. 3, 5, and 6) whereas they tremendously broaden at crystal orientations in between. So, e.g., for Rb(1) the incommensurate spectrum reaches a width of about 2 MHz at a temperature of 43 °C. The satellite singularities of Rb(2) depend on the crystal orientation qualitatively in the same manners near the orientations $\mathbf{a}\|\mathbf{H}_0$ and $\mathbf{b}\|\mathbf{H}_0$. The gaps which are obvious in the sequences of the data points of Figs. 10 and 11 are caused by the fact that at those orientational regimes the satellite transitions are superimposed on the much stronger central transition and, therefore, are not detectable. Because of this reason also the behavior of the Rb(1) satellite singularities near the crystal orientation $\mathbf{a}\|\mathbf{H}_0$ cannot be clarified exactly (Fig. 10).

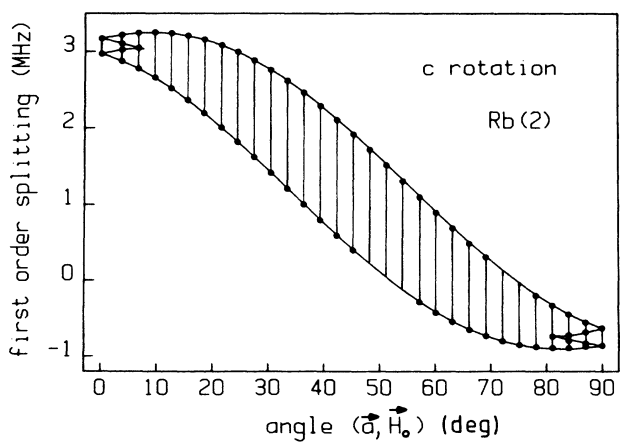


FIG. 11. Same as Fig. 10, now for Rb(2).

## IV. GENERAL SYMMETRY CONSIDERATIONS FOR THE IC PHASE

The following considerations do not depend on any model for the EFG and hold in the entire IC phase. They are based only on the periodicity of the IC modulation and on the symmetry of the IC phase as given by the corresponding superspace group. Since this group is identical for RZB and RZC, the considerations are valid for both substances.

For the IC phase of $K_2SeO_4$ the superspace group $P^{Pcmn}_{ss\,\bar{1}}$ was determined[16] by considering the symmetry of the order-parameter mode.[17] $K_2SeO_4$ undergoes the same sequence N-IC-C of phase transitions as RZB (RZC) the N and C phases being isomorphous to those of RZB (RZC). Therefore, the IC phase of RZB (RZC) is associated with the same superspace group $P^{Pcmn}_{ss\,\bar{1}}$ This superspace group was also used in Ref. 18 for RZB. As it will be shown , the assignment of this superspace group to the IC phase of RZB is in fact in accordance with our experimental results.

### A. Form of the EFG modulation tensor function

The EFG modulation tensor functions $\underline{V}^{\mu}(v)$ as introduced in I are related to each other by the superspace symmetry element $\{R\,|\,\mathbf{t},\tau\}$ according to (26) in I. The form of the modulation tensor function $\underline{V}^{\mu}(v)$ for one nucleus $\mu$ of the basic unit cell is only then restricted by a particular element $\{R\,|\,\mathbf{t},\tau\}$, if $\{R\,|\,\mathbf{t}\}$ keeps $\mu$ invariant in the basic structure. For the Rb nuclei this condition is only fulfilled by the element $\{\sigma_y\,|\,0\tfrac{1}{2}0,\pi\}$, which corresponds to the operation $(^{m}_{s})$ appearing in the label of the superspace group. For this case (26) in I can be written as

$$\underline{V}^{\mu}(v+\pi)=\sigma_y\underline{V}^{\mu}(v)\bar{\sigma}_y\ . \tag{2}$$

Representing as usual the EFG in the crystal reference frame, it follows

$$\begin{aligned} &V^{\mu}_{ij}(v+\pi)=V^{\mu}_{ij}(v) \quad \text{for } ij=xx,\ yy,\ zz,\ xz \\ &V^{\mu}_{ij}(v+\pi)=-V^{\mu}_{ij}(v) \quad \text{for } ij=xy,\ yz\ , \end{aligned} \tag{3}$$

where $\mu$ can represent any Rb nucleus of the basic unit cell. The condition (3) means that in the Fourier series [cf. Eqs. (12) and (18) in I]

$$V_{ij}^{\mu}(v)=V_{Nij}^{\mu}+\sum_{n=0,\pm1,\ldots} V_{nij}^{\mu}e^{inv}$$
$$=V_{Nij}^{\mu}+V_{oij}^{\mu}+\sum_{(n\geq 1)} 2\,|\,V_{nij}^{\mu}\,|\cos(nv+\Psi_{nij}^{\mu}) \quad (4)$$

for any nuclei $\mu$, only terms of even order appear for EFG components with $ij=xx, yy, zz, xz$, while for EFG components with $ij=xy, yz$, which are zero in the N phase due to the mirror plane $m_y$, only odd terms exist. These results generalize those previously obtained,[18] where special models were used for the EFG in contrast to the present approach.

### B. Degeneracies and symmetries of rotation patterns of the frequency distributions

As explained in detail in I, the degeneracies of the frequency distributions for different nuclei resulting from a superspace symmetry element $\{R\,|\,\mathbf{t},\tau\}$ in an incommensurate structure are analogous to those of the discrete frequencies for nuclei related by the three-dimensional part $\{R,\mathbf{t}\}$ in the corresponding commensurate average structure. The same analogy holds for symmetries appearing in the rotation patterns. For RZB (RZC) the symmetry of the average structure is identical with the symmetry of the N structure. Therefore, the degeneracies and rotation pattern symmetries for the frequency distributions in the IC phase correspond to those for the discrete frequencies in the $N$ phase. Accordingly, for the nuclei $\mu=1,\ldots,4$ of Rb(1) or Rb(2), respectively, there are a twofold degeneracy for any crystal orientation and a fourfold degeneracy for the $a$ and $c$ rotations and for the crystal orientations $\mathbf{a},\mathbf{b},\mathbf{c}\|\mathbf{H}_0$. Besides, there is a reflection symmetry in the $c$-rotation pattern of the IC frequency distributions with respect to the crystal orientations $\mathbf{a},\mathbf{b}\|\mathbf{H}_0$, i.e.,

$$f^{\mu}(\nu,\theta_z)=f^{\mu}(\nu,-\theta_z)\ , \quad (5)$$

where $\theta_z=\sphericalangle(\mathbf{a},\mathbf{H}_0)$ and $f^{\mu}(\nu)$ denotes a frequency distribution for any NMR transition. An analogous relation holds for the $a$ rotation. For a $b$ rotation we have

$$f^{1,2}(\nu,\theta_y)=f^{3,4}(\nu,-\theta_y),\quad \theta_y=\sphericalangle(\mathbf{c},\mathbf{H}_0)\ , \quad (6)$$

i.e. the $b$-rotation patterns $f^{1,2}(\nu,\theta_y)$ and $f^{3,4}(\nu,\theta_y)$ can be transformed into each other by a reflection with respect to the crystal orientations $\mathbf{c},\mathbf{a}\|\mathbf{H}_0$.

## V. DISCUSSION OF THE ORIENTATIONAL DEPENDENCES OF THE SPECTRA IN THE IC PHASE

### A. Present results on RZB

As explained in Sec. IV, in the case of a $c$ rotation the satellite transition frequency distributions $f^{\mu}(\nu_{\pm},\theta_z)$ coincide for symmetry related nuclei $\mu=1,\ldots,4$, labeled by Rb(1) or Rb(2), respectively. Thus, it is sufficient to consider only the two distributions $f^{\mu}(\nu_{\pm},\theta_z)$ for one $\mu$ per Rb type. In what follows, $\mu$ distinguishes between the two different Rb types. Referring to Figs. 7 and 9, we can state that the orientational dependences of the IC spectra for a $c$ rotation show the symmetry with respect to the crystal orientations with $\mathbf{a},\mathbf{b}\|\mathbf{H}_0$ as predicted by (5).

The frequency-modulation functions for the $\pm\frac{1}{2}\leftrightarrow\pm\frac{3}{2}$ satellite transitions can be expressed by

$$\nu_{\pm}^{\mu}(v)=\nu_L\mp\nu_1^{\mu}(v)+\nu_2^{\mu}(v) \quad (7)$$

where $\nu_L=\gamma H_0/2\pi$ and $\nu_1(v)$, $\nu_2(v)$ denote the modulation functions of the frequency shifts due to quadrupolar perturbation in first and second order, respectively. The dominant features of the frequency distributions are their singularities, which in the present case can be obtained according to (16) in I by

$$\left[\frac{d\nu_{\pm}^{\mu}(v)}{dv}\right]_{v=v_{s\pm}^{\mu}}=\left[\mp\frac{d\nu_1^{\mu}(v)}{dv}+\frac{d\nu_2^{\mu}(v)}{dv}\right]_{v=v_{s\pm}^{\mu}}=0\ . \quad (8)$$

Accordingly, in principle, the internal coordinates $v_{s+}^{\mu}$ and $v_{s-}^{\mu}$ of the singularities of the $\pm\frac{1}{2}\leftrightarrow\pm\frac{3}{2}$ satellite transitions differ and the second order terms $\nu_2^{\mu}(v_{s\pm}^{\mu})$ cannot be cancelled by taking the difference $\nu_+^{\mu}(v_{s+}^{\mu})-\nu_-^{\mu}(v_{s-}^{\mu})$ in contrast to the case of discrete satellite transitions for commensurate phases. On the other hand, practically, the difference $v_{s+}^{\mu}-v_{s-}^{\mu}$ should be very small and besides, $\nu_{\pm}^{\mu}(v)$ change very weakly in the neighborhood of $v_{s\pm}^{\mu}$. Therefore, the variation of the second-order term $\nu_2^{\mu}(v)$ with $v$ will be disregarded in (7) and (8), i.e., $\nu_2^{\mu}(v)$ is replaced by a constant. Consequently $v_s^{\mu}=v_{s+}^{\mu}=v_{s-}^{\mu}$ and $\Delta\nu^{\mu}(v_s^{\mu})\equiv\nu_-^{\mu}(v_s^{\mu})-\nu_+^{\mu}(v_s^{\mu})$ contains no second-order terms.

Rewriting Volkoff's formula (1) for a $c$ rotation and using the Fourier series (4) truncated after the second-order terms together with the condition (3), we obtain

$$\Delta\nu^{\mu}(v_s^{\mu},\theta_z)=[U_{0xx}^{\mu}+U_{2xx}^{\mu}\cos(2v_s^{\mu}+\Psi_{2xx}^{\mu})]\tfrac{1}{2}[1+\cos(2\theta_z)]$$
$$+[U_{0yy}^{\mu}+U_{2yy}^{\mu}\cos(2v_s^{\mu}+\Psi_{2yy}^{\mu})]\tfrac{1}{2}[1-\cos(2\theta_z)]-[U_{1xy}^{\mu}\cos(v_s^{\mu})\sin(2\theta_z)]\ , \quad (9)$$

where $U_{0ii}^{\mu}=(V_{Nii}^{\mu}+V_{0ii}^{\mu})eQ/h$, $U_{nij}^{\mu}=2\,|\,V_{nij}^{\mu}\,|\,eQ/h$ for $n=1,2$. The origin of $v$ has been defined such that $\Psi_{1xy}^{\mu}=0$, and $v_s^{\mu}$ is given by

$$\pm2[d\nu_{\pm}^{\mu}(v,\theta_z)/dv]_{v=v_s^{\mu}}=[U_{2xx}^{\mu}\sin(2v_s^{\mu}+\Psi_{2xx}^{\mu})][1+\cos(2\theta_z)]$$
$$+U_{2yy}^{\mu}\sin(2v_s^{\mu}+\Psi_{2yy}^{\mu})[1-\cos(2\theta_z)]-U_{1xy}^{\mu}\sin(v_s^{\mu})\sin(2\theta_z)=0\ . \quad (10)$$

Since the internal coordinate $v$ can be restricted to an interval of the length $2\pi$ and the highest harmonic in (10) is of the type $\sin(2v)$, there are at most four real solutions $v_s$ for (10). This is in accordance with the fact, that in our experiments at most four singularities were detected (see, e.g., Figs. 9 and 11). For $\theta_z=0°$ ($\mathbf{a}\|\mathbf{H}_0$), $\Delta\nu_s^\mu$ can be readily calculated

$$\Delta\nu^\mu(\theta_z=0°, v_s^\mu+\tfrac{1}{2}\Psi_{2xx}^\mu=0,\pi)=U_{0xx}^\mu+U_{2xx}^\mu\ ,$$
$$\Delta\nu^\mu(\theta_z=0°, v_s^\mu+\tfrac{1}{2}\Psi_{2xx}^\mu=\pi/2,3\pi/2)=U_{0xx}^\mu-U_{2xx}^\mu\ . \tag{11}$$

Analogous expressions hold for $\theta_z=90°$ ($\mathbf{b}\|\mathbf{H}_0$). Again in accordance with the experiment there are two twofold-degenerate singularities for $\mathbf{a},\mathbf{b}\|\mathbf{H}_0$. The singularities which coincide belong to nuclei shifted with respect to each other by $\pi$ along the internal coordinate $v$. The degeneration of the sigularities shows up in the spectra by a corresponding increase of intensity.

The curves in Figs. 10 and 11 are fitted according to (9) and (10). The parameters $U_{0ii}^\mu$ and $U_{2ii}^\mu$, $i=x,y$, are fixed directly by experimental data for $\theta_z=0°$, 90° according to (11), thus reducing the number of parameters for all other rotation angles $\theta_z$ to three for each Rb kind. Results are given in Table I. The parentheses for $U_{0xx}$ and $\Psi_{2xx}$ of Rb(1) indicate that these parameters can be determined from the fit of the experimental data only with a considerable uncertainty caused by a partial overlap of the central transition and the satellite transitions at small rotation angles $\theta_z$. Note that the off-diagonal elements $U_{1xy}$ are considerably larger than the main diagonal elements $U_{2ii}$. This is expected from Landau theory because different orders of the order parameter are the leading terms in the corresponding EFG expansions [cf. (33) in I]. These results are reflected by the fact that the frequency distributions considerably broaden if the crystal is rotated apart from one of the positions $\mathbf{a},\mathbf{b}\|\mathbf{H}_0$.

To illustrate the behavior of the singularities of the satellite transition frequency distributions in the case of Rb(2), in Fig. 12 $2d\nu_+(v,\theta_z)/dv$ is plotted as a function of the internal coordinate $v$ for some rotation angles $\theta_z$. The zeros of this function give the internal coordinates $v_s$ of the singularities [cf. Eq. (10)]. For $\theta_z=0°$ we have $2U_{2xx}\sin(2v+\Psi_{2xx})$. With increasing $\theta_z$ this function is more and more deformed mainly by the off-diagonal term $-U_{1xy}\sin(v)\sin(2\theta_z)$. As a consequence, two zeros collapse into one at a certain $\theta_z$ disappearing for $\theta_z$ further increased. This behavior of the zeros reflects that of the singularities.

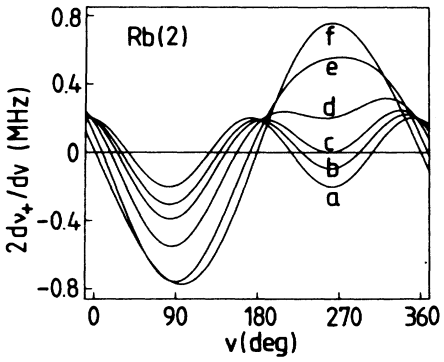


FIG. 12. $2d\nu_+(v,\theta_z)/dv$ as a function of the internal coordinate $v$ for Rb(2), $\mathbf{c}\perp\mathbf{H}_0$ and $\theta_z\sphericalangle(a,H_0)=0°$ (a), 4° (b), 7.6° (c), 15° (d), 30° (e), 45° (f). The zeroes of this function give the internal coordinates $v_s$ of the singularities [cf. Eq. (10)].

TABLE I. Parameters in (9) and (10) used for the fit curves in Figs. 10 and 11. The $U_{nij}$ are given in MHz.

| | | |
|---|---|---|
| $(U_{0xx}=0.010)$ $U_{0xx}+U_{2xx}=0.111$ | $(\Psi_{2xx}=0°)$ | Rb(1) |
| $U_{0yy}=4.291$ $U_{2yy}=0.127$ | $\Psi_{2yy}=180°$ | |
| $U_{1xy}=1.055$ | $\Psi_{1xy}=0°$ | |
| $U_{0xx}=3.067$ $U_{2xx}=0.101$ | $\Psi_{2xx}=106°$ | Rb(2) |
| $U_{0yy}=-0.748$ $U_{2yy}=0.115$ | $\Psi_{2yy}=310°$ | |
| $U_{1xy}=0.760$ | $\Psi_{1xy}=0°$ | |

As Figs. 10 and 11 show, (9) and (10) with the parameters given in Table I fit excellently to our experimental data. This means that a Fourier series of the type (4) including terms up to the second order is necessary for describing the experimental data. This Fourier series for the EFG can be connected to that of the atomic (ionic) displacements by a Taylor expansion of the EFG in terms of the displacements. As we have shown in I, according to Landau theory, an EFG Fourier series neglecting terms of third and higher order contains in principle in addition to the Fourier terms for the displacements of first order (primary or order parameter mode) also those of zeroth and second-order (secondary modes). Thus, according to our experiments, zero and second-order displacements can be of some importance. Up to now, they have been disregarded in the NMR literature, even if an EFG Taylor expansion including terms up to the second order was applied.

### B. Comparison with previous results

In a previous work[1,19] the $^{87}$Rb satellite spectra in RZC were investigated. In Fig. 5 of Ref. 1 the orientational dependences of the upper frequency satellite transition are presented for (i) Rb(1) near $\mathbf{b}\|\mathbf{H}_0$ and (ii) Rb(2) near $\mathbf{a}\|\mathbf{H}_0$ for a $c$ rotation in the upper IC phase ($T_i-T\approx 20$ K). Comparing these results with those reported above for RZB, a qualitative correspondence can be realized for the case (ii), while for the case (i) a discrepancy becomes obvious, which can be sketched roughly as follows. There are twice as many singularities for RZC than for RZB and the rotational behavior of the RZC singularities can be transformed into that of the RZB singularities in a qualitative sense by taking the mean value of the frequencies of certain RZC singularity pairs. As we know by now and have proved by experiment too, the RZC crystal was not adjusted exactly with its $c$ axis perpendicular to the magnetic field $H_0$. In fact, the qualitative discrepancy just mentioned is removed, if the crystal is orientated as accurately as needed. Accordingly, the RZC spectra shown in Fig. 5 of Ref. 1 reflect the fact that the fourfold degenera-

cy of the satellite transition frequency distributions for a $c$ rotation (see Sec. IV B) is removed due to the misorientation of the $c$ axis of the RZC crystal. Consequently, there are two frequency distributions instead of one.

We note that also some of the temperature dependences of the RZC satellite transitions at special crystal orientations ($\mathbf{a},\mathbf{b},\mathbf{c}\|\mathbf{H}_0$) described in Ref. 1 do not show the necessary degeneracy because of some misorientation of the crystal, to which the satellite transitions are very sensitive. The qualitative discrepancies between the temperature dependence of the Rb(1) satellite transitions at $\mathbf{b}\|\mathbf{H}_0$ for RZC and RZB must also be attributed to that fact. The central transitions of the $^{87}$Rb nuclei in RZB and RZC are much less affected if the crystal is not orientated exactly in the way wanted. According to available data previously obtained,[3–5,19,20] the rotation patterns of the central transitions in the IC phases are also compatible with the degeneracies and symmetries derived in Sec. IV. Of course, the smaller sensitivity and resolution of these experiments must be taken into consideration. Especially in the case of a $b$ rotation for RZC (Ref. 19) the symmetry relation (6) becomes obvious.

In previous NMR studies on the IC phases of RZB or RZC, dealing with the $^{87}$Rb central transition,[3–5] a so-called "local" approximation[12] has been applied to the EFG. As we explained in detail in I, this model only then holds for the general case, if the EFG expansion in terms of the atomic (ionic) displacements includes only one displacement (usually that one is considered which belongs to the nucleus under observation) of one harmonic (the first one) in one direction. Using the internal coordinate $v$, the EFG expansion truncated after the second-order terms writes according to the "local" model in the sinusoidal regime as [cf. Eq. (19) of I]

$$V_{ij}^{\mu}(v)=V_{Nij}^{\mu}+T_{1ij}^{\mu}\cos(v+\varphi_0)+T_{2ij}^{\mu}\cos^2(v+\varphi_0)\ . \tag{12}$$

The restrictions which this expansion imposes on the Fourier series (4) are given in (21) and (22) of I. Thus, the condition

$$\Psi_{2ii}^{\mu}=2\Psi_{1xy}^{\mu}(+\pi) \tag{13}$$

should be fulfilled. Accordingly, the $c$-rotation pattern for $\Delta\nu^{\mu}(v_s^{\mu},\theta_z)$ as defined by (9) and (10) should look like that of the fit curve for Rb(1) (see Fig. 10 and Table I). The orientational dependence $\Delta\nu^{\mu}(v_s^{\mu},\theta_z)$ for Rb(2) markedly differs from this behavior (Fig. 11). The "local" model using expansion terms up to the second-order results in a degeneration of two singularities in some ranges of rotation angles near $\theta_z=0°$ and $\theta_z=90°$. For Rb(2) this degeneration is clearly removed and, correspondingly, condition (13) is not fulfilled (cf. Table I). Also for Rb(1) this degeneracy is not realized exactly as indicated by the broadening of the left singularity in Fig. 8 for, e.g., $\theta_z=90°-7.5°$. At lower temperatures the splitting into two singularities can be clearly observed (Fig. 7).

There is still a general argument to show that the "local" model is in conflict with our experimental results, even if the symmetry condition (3) is disregarded and expansion terms of any order are taken into account. For this case, using (9) and (10) correspondingly modified, one obtains singularities whose rotational dependences $\Delta\nu(v_s,\theta_z)$ should be of a $\cos(2\theta_z\pm\delta)$ type. As Fig. 11 shows, for Rb(2) there are no $\Delta\nu(v_s,\theta_z)$ which could be fitted by such a function over the whole range of rotation angles.

The contradictions resulting from the "local" EFG model are not surprising, if one remembers the restrictions mentioned above. Since the EFG at the site of a nucleus is caused by the environment of this nucleus, really the displacement of the nucleus itself and the displacements of neighboring atoms (ions) have an influence of the same order of magnitude on the EFG modulation. (These displacements can be completely out of phase.) Thus, for a general model, it is not plausible to consider one displacement but disregard the rest. In addition, even if one would do so, all harmonics up to the second order of this one displacement should be included in the EFG expansion which generally then again would differ from the local EFG expansion (12). We stress that the measured rotational dependence $\Delta\nu(v_s,\theta_z)$ for Rb(1) does not prove the validity of the "local" model for this special case because of the considerable uncertainty in determining the value of $\Psi_{2xx}$ (cf. Table I). Besides, all other conditions included in (21) and (22) in I should have to be checked (see also Sec. VI).

According to the "local" model, certain parts of the IC frequency distributions could be associated with certain parts of the first harmonic of the modulation of the one displacement taken into account. This actually was done in previous works.[3–5] For example, the two singularities whose rotational dependences should be of the $\cos(2\theta\pm\delta)$ type (see above) should be associated with the maxima and minima of the modulation specified above. It follows from the preceding discussion, that such an assignment is not possible.

## VI. DISCUSSION OF THE TEMPERATURE DEPENDENCES

For the crystal orientation $\mathbf{a}\|\mathbf{H}_0$ the frequency modulation function for the $\pm\frac{1}{2}\leftrightarrow\pm\frac{3}{2}$ satellite transitions is given by[21]

$$\nu_{\pm}^{\mu}(v,\mathbf{a}\|\mathbf{H}_0)=\nu_L^{\mu}+\left\{\mp\frac{1}{2}V_{xx}^{\mu}(v)+\frac{1}{6\nu_L}\{[V_{xy}^{\mu}(v)]^2+[V_{xz}^{\mu}(v)]^2\}\right\}\frac{eQ}{h}\ . \tag{14}$$

Introducing the local EFG expansion (12) and using condition (3), this relation contains only terms of even order in $\cos(v+\varphi_0)$. Consequently, one singularity would coincide with the frequency $\nu_{N\pm}^{\mu}$ of the N phase and therefore would be independent of temperature (cf. Ref. 12). The same argument, of course, holds for the other special crystal orientations $\mathbf{b},\mathbf{c},\|\mathbf{H}_0$. As Figs. 2–6 show, there is no such singularity and thus the "local" model fails again. Strictly speaking, since the frequencies of the satellite transitions for a fixed orientation can vary with temperature in the N phase, one should define $\nu_{N\pm}^{\mu}$ as the extrapolations of these temperature dependences into the IC

phase. According to our measurements these temperature dependences are too weak to remove the contradiction between the "local" model and our experimental results just mentioned.

Using the approximation introduced on deriving (9) and (10) we obtain from (14) for the $\frac{1}{2}\leftrightarrow\frac{3}{2}$ satellite transition

$$\nu^{\mu}(v)=\nu_N^{\mu}+\nu_0^{\mu}-\tfrac{1}{2}U_{2xx}^{\mu}\cos(2v+\Psi_{2xx}^{\mu}) , \tag{15}$$

where $\nu_0$ includes the contributions of all homogeneous terms $V_{0ij}^{\mu}$. Then according to (8) the singularities of the frequency distribution are

$$\nu_{1/2}^{\mu}=\nu_N^{\mu}+\nu_0^{\mu}\pm\tfrac{1}{2}U_{2xx}^{\mu} . \tag{16}$$

Using Landau theory (see, e.g., I) we consequently obtain

$$|\nu_1^{\mu}-\nu_2^{\mu}|=U_{2xx}^{\mu}=a\rho^2+b\rho^4+\cdots , \tag{17}$$

where $a$ and $b$ are constants and $\rho$ is the amplitude of the order parameter. The missing of odd powers of $\rho$ in (17) originates in the symmetry condition (3). Analogous expressions hold for the $-\frac{1}{2}\leftrightarrow-\frac{3}{2}$ satellite and for the other special crystal orientations $\mathbf{b},\mathbf{c}\|\mathbf{H}_0$.

It follows that at these special orientations for each Rb type and both satellite transitions the frequency distance of the two singularities varies with temperature according to $\rho^2(T)$ as long as terms of higher order in $\rho$ can be neglected. As it can be seen from (33) in I, in the Fourier series (4) for the EFG terms up to the order $n$ have to be taken into account, if $n$ is the power of $\rho$ to be considered. The $c$ rotation discussed in Sec. V could be fitted applying an EFG Fourier series including terms up to the second order. It was recorded about 30 K below $T_i$. Therefore, in a temperature range of at least 30 K below $T_i$ the $\rho^4$ terms in (17) should be unimportant.

In literature often a temperature dependence $\rho(T)\propto(T_i-T)^{\beta}$ is assumed.[3–5,12,22–24] Checking the validity of this power law by experimental data is quite sensitive to the fixing of $T_i$. Our data presently available do not allow to determine $T_i$ as accurately as necessary. Therefore, we omit here a detailed discussion of this point. Choosing $T_i$ such that the power law holds for a maximal temperature range, we could fit our data by $2\beta=0.83\pm0.02$ for Rb(1), $\mathbf{b}\|\mathbf{H}_0$, $2\beta=0.84\pm0.03$ for Rb(2), $\mathbf{a}\|\mathbf{H}_0$, $2\beta=0.86\pm0.02$ for Rb(2), $\mathbf{b}\|\mathbf{H}_0$. These values for $2\beta$ are valid in a temperature range between $T_i$ and temperatures about 30–40 K below $T_i$. At lower temperatures the satellite frequency distances become distinctly broader than predicted by the $(T_i-T)^{2\beta}$ law (Fig. 13). The values for $2\beta$ do not differ much for the three cases investigated. On the other hand, the deviation from the value $\beta=0.35\pm0.03$ previously obtained by NMR measurements on the $^{87}$Rb central transition[4] is obvious. In addition, in Ref. 4 the power law was fitted over a temperature range of about 100 K, this is about two thirds of the entire IC phase.

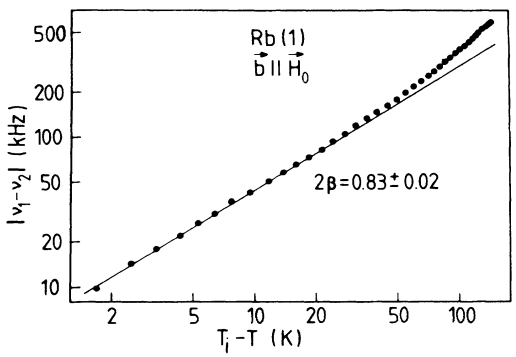


FIG. 13. Double logarithmic plot of the frequency distance $|\nu_2-\nu_1|$ of the singularities given in Fig. 5 vs $T_i-T$.

Another discrepancy between our experimental results and those presented in Ref. 4 arises in the temperature range between $T_i$ and about 10 K below $T_i$. Therein it is reported, that in this temperature range an additional line appears between the two edge singularities at frequencies, at which in the N phase the discrete line is observed. As argued in a following work,[25] this additional line results from a floating of the modulation waves, which completely averages out the IC frequency distribution. We did not observe such an additional line (see Fig. 2) and so we can exclude such a strong floating of the modulation waves at least for this broad temperature range below $T_i$. This cannot be attributed to a minor quality of the crystal we used because of the quality of the satellite spectra presented here. Also in our previous studies[1,19] on RZC we could not find any hint on such a strong floating.

On approaching the lock-in transition at $T_c$ from above, in addition to the two edge singularities other maxima of intensity appear in the frequency distributions (cf. Figs. 2–5). Since the additional maxima of intensity which can be seen in approximately the middle part of the IC spectra merge into the middle C line of the C phase, these centers of intensity may be attributed reasonably to nearly commensurate regions in the IC phase. According to Landau theory these are regions where the phase of the order parameter changes weakly (see, e.g., Ref. 26). This is the usual interpretation which was also applied in the case of NMR $^{87}$Rb central transition studies on RZB and RZC.[4,13] However, on going into the IC phase from $T_c$, for Rb(2) $\mathbf{a}\|\mathbf{H}_0$ we do not observe only a broadening of those lines which represent approximately commensurate regions, as it is usual for the central transition, but more complicated spectra (Fig. 2). We stress that this fact cannot be attributed to a misorientation of the crystal because we observe three sharp fourfold degenerate lines below $T_c$.

As the centers of intensity in the middle part of the IC spectra represent nearly commensurate regions, correspondingly, the outer intensity maxima merging into C lines must contain such contributions of nearly commensurate regions, too. Looking at the left edge intensity in Fig. 4 one sees that the amplitude of the right part of that edge intensity partially split decreases (compared with that of the left part) at increasing temperature simultaneously with the amplitude of the intensity in the middle of the spectrum. Thus, the left part of the left edge intensity represents incommensurate regions or discommensurations (phase solitons), i.e. regions where the phase of the order parameter changes strongly, and the right part approximately commensurate ones. As our experimental results show, both edge singularities originating from the

discommensurations nearly cannot be distinguished from the outer intensity maxima arising from almost commensurate regions. This seems to indicate that the amplitude of the order parameter is smaller in the discommensurations than in the nearly commensurate regions[27] and, thus, the constant amplitude approximation does not hold in this temperature region. Such a decrease of the order parameter amplitude in the discommensurations is also predicted by numerical treatments of the Landau potentials.[26]

As the line shapes and the intensity ratio 1:1:1 (cf. Sec. III B) of the three lines detected below $T_c$ show, incommensurate contributions below $T_c$, if existing at all, must be small, i.e., the soliton density $n_s \approx 0$ below $T_c$. This is in contrast to the rather high value $n_s \approx 0.5$ ($T < T_c$) recently redetermined[11] from the $^{87}$Rb central transition studies[4] already mentioned. This latter result would mean that nearly one half of the crystal is not commensurate below $T_c$. One reason for this rather high $n_s$ value, also stated by the authors themselves, could be a rather high impurity concentration in the RZB crystals.

The frequencies of each of the three discrete C lines measured below $T_c$ for one Rb kind of the N phase show an approximately linear temperature dependence which is the stronger the farther the corresponding distance from the frequency of the N line detected above $T_i$. Hence these temperature dependences presumably indicate a further increase of the amplitude of the commensurate modulation in the C phase on cooling. This interpretation is confirmed by investigations of the spontaneous polarization $P_s$ on RZB.[28,29] According to these measurements, $P_s$ still increases below $T_c$.

## ACKNOWLEDGMENTS

The authors are indebted to the Deutsche Forschungsgemeinschaft (Sonderforschungsbereich 130) and to CAICYT (Spain), the Direccion General de Politica Cientifica (Spain). We thank A. Klöpperpieper for growing and preparing the crystals and E. Schneider for stimulating discussions and experimental assistance.

[1]E. Schneider and J. Petersson, Z. Phys. B **46**, 169 (1982).
[2]J. M. Perez-Mato, R. Walisch, and J. Petersson, preceding paper, Phys. Rev. B **35**, 6529 (1987).
[3]V. Rutar, J. Seliger, B. Topič, R. Blinc, and I. P. Aleksandrova, Phys. Rev. B **24**, 2397 (1981).
[4]V. Rutar, F. Milia, B. Topič, R. Blinc, and Th. Rasing, Phys. Rev. B **25**, 281 (1982).
[5]I. P. Aleksandrova, S. Grande, Yu. N. Moskvich, A. I. Krieger, and V. A. Koptsik, Phys. Status Solidi B **115**, 603 (1983); I. P. Aleksandrova, Yu. N. Moskvich, S. Grande, and A. I. Krieger, Zh. Eksp. Teor. Fiz. **85**, 1335 (1983) [Sov. Phys.—JETP **58**, 774 (1983)].
[6]R. Walisch, E. Schneider, and J. Petersson, *Proceedings of the 22nd Congress Ampere, Zürich (1984),* edited by K. A. Muller, R. Kind, and J. Roos (Springer-Verlag, Berlin, 1985), p. 34.
[7]J. Dolinšek, S. Zumer, and R. Blinc, *Proceeding of the 22nd Congress Ampere, Zürich (1984),* Ref. 6.
[8]J. Pirnat, J. Lužnik, and Z. Trontelj, *Proceedings of the 22nd Congress Ampere, Zürich (1984),* Ref. 6.
[9]B. Müller, J. Petersson, and R. Walisch, Proceedings of the 23rd Congress Ampere, 134, Rome (1986) (unpublished).
[10]J. Dolinšek and R. Blinc, Z. Naturforsch. **41a**, 265 (1986).
[11]R. Blinc, V. Rutar, B. Topič, F. Milia, and Th. Rasing, Phys. Rev. B **33**, 1721 (1986).
[12]R. Blinc, J. Seliger, and S. Zumer, J. Phys. C **18**, 2313 (1985).
[13]J. Petersson and E. Schneider, Z. Phys. B **61**, 33 (1985).
[14]C. J. de Pater, Acta Crystallogr. Sect. B **35**, 299 (1979).
[15]G. M. Volkoff, H. E. Petch, and D. W. L. Smellie, Can. J. Phys. **30**, 270 (1952).
[16]A. Janner and T. Janssen, Acta Crystallogr. Sect. A **36**, 399 (1980).
[17]M. Iizumi, J. D. Axe, G. Shirane, and K. Shimaoka, Phys. Rev. B **15**, 4392 (1977).
[18]B. W. van Beest, A. Janner, and R. Blinc, J. Phys. C. **16**, 5409 (1983).
[19]E. Schneider, Ph.D. thesis, University of Saarbrücken (1983).
[20]R. Walisch, Diploma thesis, University of Saarbrücken (1984).
[21]G. M. Volkoff, Can. J. Phys. **31**, 820 (1953).
[22]C. J. de Pater and C. van Dijk, Phys. Rev. B **18**, 1281 (1978).
[23]H. Mashiyama, J. Phys. Soc. Jpn. **50**, 2655 (1981).
[24]H.-G. Unruh and J. Strömich, Solid State Commun. **39**, 737 (1981).
[25]R. Blinc, D. C. Ailion, P. Prelovšek, and V. Rutar, Phys. Rev. Lett. **50**, 67 (1983).
[26]Y. Ishibashi, J. Sugiyama, and A Sawada, J. Phys. Soc. Jpn. **50**, 2500 (1981), and references therein.
[27]R. Blinc, P. Prelovšek, and R. Kind, Phys. Rev. B **27**, 5404 (1983).
[28]C. J. de Pater, Phys. Status Solidi A **48**, 503 (1978).
[29]S. Sawada, T. Yamaguchi, Y. Shiroishi, A. Yamamoto, and M. Takashige, J. Phys. Soc. Jpn. **50**, 3677 (1981).